IOP Publishing | Astro Ltd Laser Physics

Laser Phys. 26 (2016) 095004 (6pp) doi:10.1088/1054-660X/26/9/095004

# A $Cr^{4+}$:YAG passively Q-switched Nd:$YVO_4$ microchip laser for controllable high-order Hermite–Gaussian modes

**Jun Dong[1], Yu He[1], Sheng-Chuang Bai[1], Ken-ichi Ueda[2] and Alexander A Kaminskii[3]**

[1] Department of Electronics Engineering, School of Information Science and Engineering, Xiamen University, Xiamen 361005, People's Republic of China
[2] Institute for Laser Science, University of Electro-Communications, 1-5-1 Chofugaoka, Chofu, Tokyo 182–8585, Japan
[3] Institute of Crystallography, Russian Academy of Sciences, Leninsky Prospekt 59, Moscow 119333, Russia

E-mail: jdong@xmu.edu.cn

Received 19 May 2016, revised 26 June 2016
Accepted for publication 27 June 2016
Published 29 July 2016

**Abstract**

A nanosecond, high peak power, passively Q-switched laser for controllable Hermite–Gaussian (HG) modes has been achieved by manipulating the saturated inversion population inside the gain medium. The stable HG modes are generated in a $Cr^{4+}$:YAG passively Q-switched Nd:$YVO_4$ microchip laser by applying a tilted pump beam. The asymmetrical saturated inversion population distribution inside the Nd:$YVO_4$ crystal for desirable HG modes is manipulated by choosing the proper pump beam diameter and varying pump power. A $HG_{9,8}$ mode passively Q-switched Nd:$YVO_4$ microchip laser with average output power of 265 mW has been obtained. Laser pulses with a pulse width of 7.3 ns and peak power of over 1.7 kW working at 21 kHz have been generated in the passively Q-switched Nd:$YVO_4$ microchip laser.

Keywords: Hermite–Gaussian mode, beam characteristics, microchip laser, passively Q-switched, solid-state lasers, laser-diode pumped

(Some figures may appear in colour only in the online journal)

## 1. Introduction

Lasers with special field distributions, such as high-order transverse modes, have gained more attention in recent years, as high-order transverse mode lasers have potential applications in the manipulation of particles, optical trapping, optical guiding, the formation of versatile vortices, and so on [1, 2]. The Hermite–Gaussian (HG) mode generated in a resonator has specific characteristics suited to various applications compared to those obtained with optical methods [3]. Compared to gas lasers and semiconductor lasers, laser-diode pumped solid-state lasers are more suitable for generating stable transverse modes with a desirable transverse amplitude distribution [4–7]. HG modes have been generated in laser-diode end-pumped solid-state lasers [3, 8]. Recently, the HG or Ince–Gaussian laser beams generated in laser-diode pumped solid-state lasers have been used to form various vortex beams by adopting a mode converter [9–11]. However, the practical applications of various vortex beams are limited by the complicated laser systems. Recently, on-demand laser modes such as Laguerre–Gaussian, HG, flat-top, and Airy modes have been successfully generated in a laser-diode pumped digital laser by replacing the output coupler by a computer-controlled spatial light modulator [12]. However, these lasers work in the continuous-wave and their output power is only several milliwatts. The potential applications of these lasers are limited by the low output power and low optical conversion efficiency. High peak power and high repetition rate HG mode lasers are favorable for the large capacity required by quantum computation, high resolution optical trapping, and manipulating micro-particles. A higher-order Ince–Gaussian mode laser with over 1 kW peak power and a nanosecond pulse width has been demonstrated in a laser-diode end-pumped Cr,Nd:YAG self-Q-switched microchip laser by applying a tilted pump beam [13]. Complex transverse patterns have been achieved in laser-diode end-pumped Cr,Nd:YAG self-Q-switched lasers by moving the Cr,Nd:YAG crystal along the pump beam direction [14]. Because the Nd:$YVO_4$ crystal has a high absorption coefficient at pump wavelength of 808 nm, a large emission cross section, and stable physical and chemical properties, laser-diode end-pumped Nd:$YVO_4$ microchip lasers are widely used to generate high-order transverse modes [9, 15–18]. Highly efficient, high peak power, passively Q-switched lasers with a $Cr^{4+}$:YAG crystal as the saturable absorber have been demonstrated [19–21]. In addition to its excellent properties, such as a high damage threshold, simplicity, and low cost, the $Cr^{4+}$:YAG crystal also works as a spatially dynamic transmission filter in passively Q-switched lasers [22–25]. Therefore, desired transverse laser modes can be excited in passively Q-switched lasers by introducing mode discrimination with the $Cr^{4+}$:YAG crystal. Very recently, various high-order transverse modes have been demonstrated in a laser-diode end-pumped passively Q-switched Nd:$YVO_4$ microchip laser by changing the position of the Nd:$YVO_4$ crystal along the pump beam direction [26]. The saturated inversion population distribution inside the Nd:$YVO_4$ crystal has been manipulated to achieve controllable transverse laser modes. Stable HG modes have been obtained in a passively Q-switched Nd:$YVO_4$ microchip laser when the Nd:$YVO_4$ crystal is positioned far away from the focused pump beam spot. However, the indices of these HG modes are low and their output power is only tens of milliwatts, because a large pump beam area is applied and the incident pump power is set to constant. Also, the pulse energy and peak power of the HG mode generated in a passively Q-switched Nd:$YVO_4$ microchip laser are only 2 $\mu$J and 130 W when the Nd:$YVO_4$ crystal is positioned close to focus lens [26]. High-order HG mode generation in a laser-diode pumped passively Q-switched Nd:$YVO_4$ microchip laser strongly depends on the saturated inversion population distribution provided by the pump power when the pump beam waist and the incident angle of the pump beam are properly selected. Therefore, the effect of the pump power on the generation of high-order HG modes in a passively Q-switched Nd:$YVO_4$ microchip laser is worth investigating.

Here, controllable high-order HG modes have been achieved with a laser-diode pumped $Cr^{4+}$:YAG passively Q-switched Nd:$YVO_4$ microchip laser by manipulating the saturated inversion population inside the Nd:$YVO_4$ crystal. The asymmetric saturated inversion population inside the Nd:$YVO_4$ crystal for generation of the desired high-order HG modes in a passively Q-switched Nd:$YVO_4$ microchip laser has been manipulated by adjusting the pump beam area and pump power intensity of a tilted pump beam from the laser diode. Distinct high-order HG modes laser with nanosecond pulse widths and kilowatt peak powers have been achieved using the $Cr^{4+}$:YAG passively Q-switched Nd:$YVO_4$ microchip laser by controlling the input pump power.

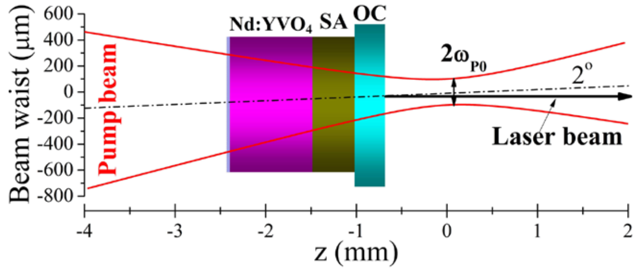


**Figure 1.** Experimental set-up for generation of high-order HG modes in a $Cr^{4+}$:YAG passively Q-switched Nd:$YVO_4$ microchip laser. SA is the saturable absorber, OC is the output coupler, $\omega_{p0}$ is the focus waist of the pump beam, and $z$ is the position of the Nd:$YVO_4$ crystal along the pump beam direction.

## 2. Experimental details

The experimental set-up of the laser-diode pumped $Cr^{4+}$:YAG passively Q-switched Nd:$YVO_4$ microchip laser for generating high-order HG laser modes is shown in figure 1 and is similar to that in [26]. The pump source is an 808 nm fiber-coupled laser diode. The numerical aperture and the core diameter of the fiber are 0.22 and 400 $\mu$m, respectively. Two focus lenses with 8 mm and 15 mm focal lengths were used to collimate and focus the pump beam. The diameter ($2\omega_{p0}$) at the pump beam focus spot after optical coupling of system was 200 $\mu$m. The pump beam was tilted 2 degrees away from the laser beam. A 1 mm thick a-cut Nd:$YVO_4$ crystal was used as the gain medium. The $Nd^{3+}$ ion doping concentration in the Nd:$YVO_4$ crystal was 1 at.%. Anti-reflection at 808 nm and high-reflection at 1064 nm were coated on one surface of the Nd:$YVO_4$ crystal to act as the rear cavity mirror. Anti-reflection at 1064 nm was coated on the other surface of Nd:$YVO_4$ crystal to reduce the intracavity loss. The saturable absorber is a 0.5 mm thick $Cr^{4+}$:YAG crystal with an initial transmission of 88.5%. The $Cr^{4+}$:YAG crystal was sandwiched between the Nd:$YVO_4$ crystal and the plane-parallel output coupler with reflection of 90% at 1064 nm. The cavity length is 1.5 mm. HG modes were generated when the Nd:$YVO_4$ crystal was moved far away from the focus spot based on the experimental results for generating various transverse laser modes in passively Q-switched Nd:$YVO_4$ microchip lasers [26]. For generating high-order HG transverse laser modes in a passively Q-switched laser, the Nd:$YVO_4$ crystal was positioned close to the focus lens, and the rear surface of the Nd:$YVO_4$ crystal was 2.4 mm away from the focus beam waist. The incident pump beam diameter on the rear surface of the Nd:$YVO_4$ crystal was measured to be about 1.1 mm.

Figure 2 shows the variation of the saturated inversion population distribution inside the Nd:$YVO_4$ crystal as a function of the tilted angle ($\theta$) of the pump beam when the Nd:$YVO_4$ crystal is positioned 2.4 mm away from the pump beam focus spot (as shown in figure 1). An incident pump power of 6.5 W from the laser diode was used for calculations. The saturated inversion population is symmetrically distributed along the pump beam direction when the pump beam is normally incident on the

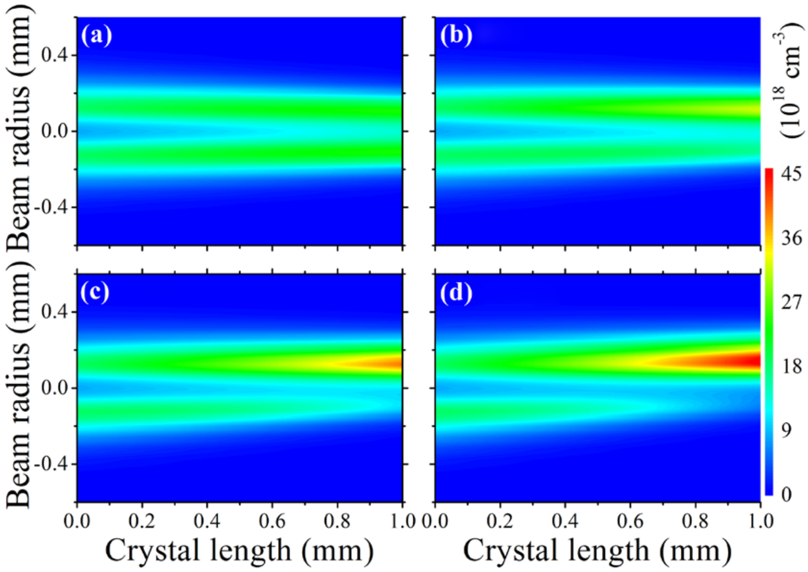


**Figure 2.** The radial saturated inversion population distribution inside the Nd:$YVO_4$ crystal as a function of the thickness of the Nd:$YVO_4$ crystal at different tilted angles ($\theta$). The Nd:$YVO_4$ crystal is positioned close to the focus lens and the rear surface of the Nd:$YVO_4$ crystal is 2.4 mm away from the focus spot of the pump beam. (a) $\theta = 0°$, (b) $\theta = 2°$, (c) $\theta = 4°$, and (d) $\theta = 6°$.

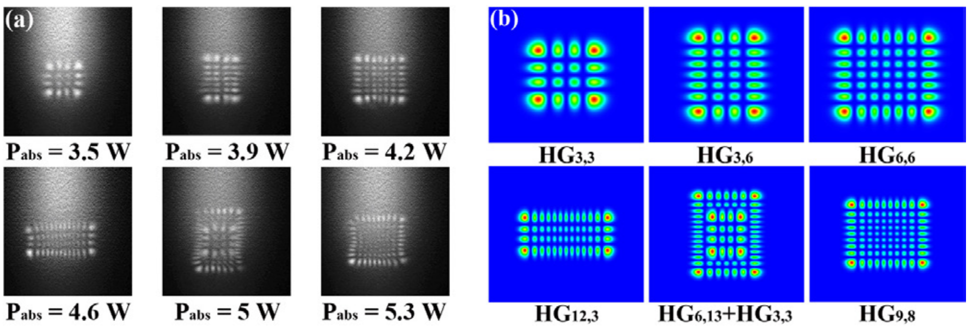


**Figure 3.** (a) High-order HG mode transverse distribution obtained in a passively Q-switched Nd:$YVO_4$ microchip laser at different absorbed pump power levels. (b) The numerical simulated results corresponding to the observed HG mode transverse distribution in (a).

Nd:$YVO_4$ crystal, as shown in figure 2(a). The saturated inversion population inside the Nd:$YVO_4$ crystal has a characteristic of minima along the pump beam axis and two maxima away from the pump beam axis. The saturated inversion population increases with the thickness of the Nd:$YVO_4$ crystal. The symmetrical saturated inversion population distribution is broken when the incident pump beam is tilted away from the normal pump beam direction, as shown in figures 2(b)–(d). The saturated inversion population increases with the tilted angle of the incident pump beam. The highest saturated inversion population shifts close to the exit surface of the Nd:$YVO_4$ crystal with the tilted angle of the pump beam. The saturated inversion population close to the exit surface of the Nd:$YVO_4$ crystal is more asymmetrically distributed with the tilted angle of the pump beam. The symmetric saturated inversion population is slightly broken when the pump beam is incident on the Nd:$YVO_4$ crystal with a 2 degree tilted angle (as shown in figure 2(b)), which is more suitable for HG mode generation. Therefore, a 2 degree tilted angle for the laser-diode pump beam is used, and the saturated inversion population inside the Nd:$YVO_4$ crystal is manipulated by adjusting the incident pump power in a high-order HG mode passively Q-switched microchip laser.

## 3. Results and discussion

When the tilted angle of the incident pump beam is set to 2 degrees and the position of the Nd:$YVO_4$ crystal along the pump beam is set to 2.4 mm from the focus spot of the pump beam, the generation of HG laser modes in the passively Q-switched Nd:$YVO_4$ microchip laser strongly depends on the applied pump power. The absorbed pump power threshold of the $Cr^{4+}$:YAG passively Q-switched Nd:$YVO_4$ microchip laser was 2.5 W owing to the large pump beam diameter of 1.1 mm applied in the experiments for HG laser mode generation. A laser beam quality analyzer (Thorlabs BC106-VIS) was used to monitor and record the output laser beam profile. The passively Q-switched Nd:$YVO_4$ microchip laser oscillated in the fundamental mode ($TEM_{00}$) when the absorbed pump power was lower than 3 W. Stable oscillation of high-order HG modes was achieved when the absorbed pump power was higher than 3 W. The $HG_{3,0}$ mode laser beam was obtained when the absorbed pump power was in the range from 3 W to 3.3 W. High-order HG modes were generated in the $Cr^{4+}$:YAG passively Q-switched Nd:$YVO_4$ microchip laser when the absorbed pump power was higher than 3.3 W. The transition of the HG laser modes with

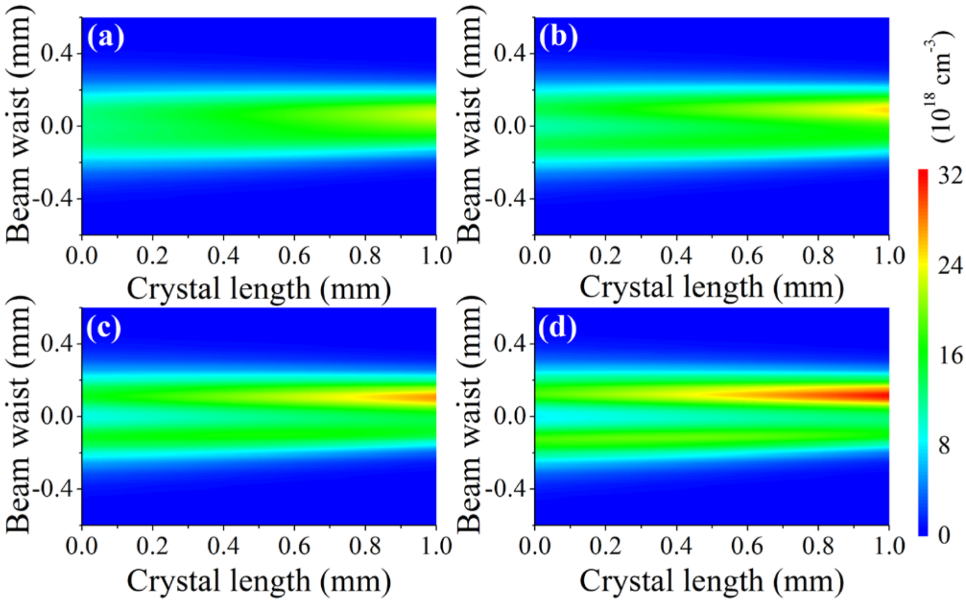


**Figure 4.** The variation of the saturated inversion population along the thickness and radius of the $Nd:YVO_4$ crystal under different absorbed pump power levels, (a) $P_{abs} = 2.8$ W, (b) $P_{abs} = 3.5$ W, (c) $P_{abs} = 4.2$ W, and (d) $P_{abs} = 5.3$ W.

pump power in the passively Q-switched $Nd:YVO_4$ microchip laser was sudden and abrupt. The indices $(m,n)$ of the HG modes generated in the passively Q-switched $Nd:YVO_4$ microchip laser increase with the pump power. The HG modes obtained in the passively Q-switched $Nd:YVO_4$ microchip laser remained stable in a certain pump power range. The $HG_{3,3}$ mode oscillated when the absorbed pump power was varied from 3.3 W to 3.6 W. The $HG_{3,6}$ mode was generated when the absorbed pump power was changed from 3.6 W to 4.1 W. The $HG_{6,6}$ mode was generated when the absorbed pump power was increased from 4.1 W to 4.4 W. The $HG_{12,3}$ mode was generated when the absorbed pump power was in the range from 4.4 W to 4.8 W. The $HG_{6,13}$ and $HG_{3,3}$ modes oscillated simultaneously when the absorbed pump power was in the range from 4.8 W to 5.1 W. A $HG_{9,8}$ mode laser was generated when the absorbed pump power was higher than 5.1 W. Figure 3 shows the observed $HG_{m,n}$ mode transverse distribution of the $Cr^{4+}$:YAG passively Q-switched $Nd:YVO_4$ microchip laser at different absorbed pump power levels, together with the corresponding numerical calculation of the observed HG mode transverse distribution. The oscillation of high-order HG laser modes in the $Cr^{4+}$:YAG passively Q-switched $Nd:YVO_4$ microchip laser was attributed to the asymmetric pump power distribution inside the $Nd:YVO_4$ crystal from applying a tilted large diameter pump beam incident on the gain medium. The pump power dependent asymmetric saturated inversion population distribution inside the $Nd:YVO_4$ crystal induced by the slightly tilted pump beam strongly governs the formation of various high-order HG modes.

The variation of the saturated inversion population distribution inside a 1 mm thick $Nd:YVO_4$ crystal along the radius and the thickness of the $Nd:YVO_4$ crystal under different pump power levels is shown in figure 4, which is calculated according to the saturated inversion population [13] by taking account into the tilted pump beam. The saturated inversion population inside the $Nd:YVO_4$ crystal exhibits a local minimum along the pump light direction and two local maximums away from the pump light direction owing to the gain guide effect induced by the gain saturation. When the $Nd:YVO_4$ crystal was positioned close to the focus lens and 2.4 mm away from the pump beam focus spot, the focus spot was outside the 1 mm thick $Nd:YVO_4$ crystal. The pump beam waist decreases with $Nd:YVO_4$ crystal length. Therefore, the pump power intensity increases along the thickness of the $Nd:YVO_4$ crystal. The saturated inversion population inside the gain medium increases along the thickness of the $Nd:YVO_4$ crystal for different pump powers. The possible laser beam area is expanded with an increase in pump power. The saturated inversion population distribution is also broadened due to the gain guiding effect under gain saturation inside the gain medium.

The incident pump power does not only determine the generation of distinct HG modes in the passively Q-switched $Nd:YVO_4$ microchip laser, but also has great effect on the laser characteristics. Figure 5 shows the variation of the average output power of a HG mode $Cr^{4+}$:YAG passively Q-switched $Nd:YVO_4$ microchip laser with absorbed pump power. The absorbed pump power threshold is 2.5 W. The high pump power threshold is caused by the large pump beam diameter used for generating high-order HG laser modes. The $TEM_{00}$ mode laser oscillates when the absorbed pump power is lower than 3 W. The HG mode laser oscillates when the absorbed pump power is higher than 3 W. The average output power increases linearly with the absorbed pump power when the laser oscillates well above the absorbed pump power threshold. The maximum average output power is 265 mW when the available absorbed pump power of 5.3 W is applied. The optical-to-optical efficiency of 5% in the high-order HG mode passively Q-switched $Nd:YVO_4$ microchip laser can be further improved by optimizing the position of the $Nd:YVO_4$ crystal along the pump beam and increasing the pump power. The average output power is not saturated within the available absorbed pump power, therefore a high average output power and high-order HG mode laser can be generated in the passively Q-switched $Nd:YVO_4$

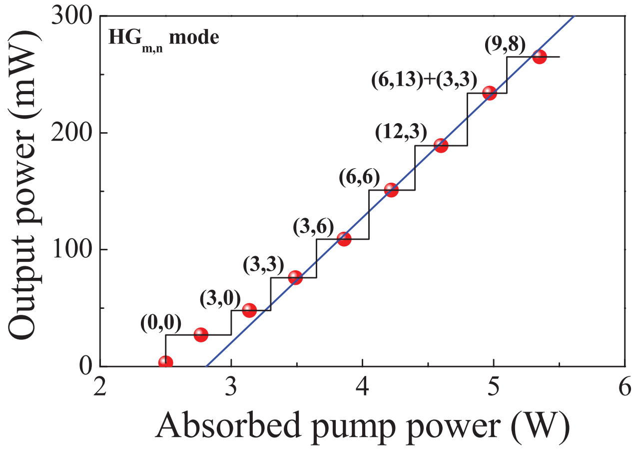


**Figure 5.** Average output power of the HG mode passively Q-switched Nd:$YVO_4$ microchip laser as a function of the absorbed pump power. The solid line is the linearly fitting of the experimental data. The step line shows the absorbed pump power range for different HG$_{m,n}$ mode oscillations. The numbers in brackets give the indices of the HG modes.

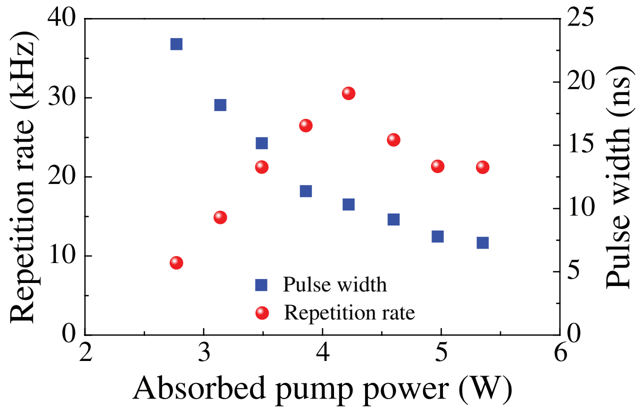


**Figure 6.** Repetition rate and pulse width of the HG mode passively Q-switched Nd:$YVO_4$ microchip laser as a function of the absorbed pump power.

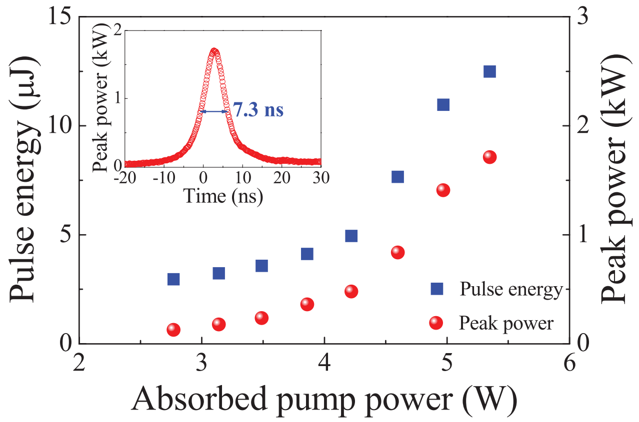


**Figure 7.** Pulse energy and peak power of the HG mode passively Q-switched Nd:$YVO_4$ microchip laser as a function of the absorbed pump power. The inset shows the pulse profile of a HG$_{9,8}$ mode laser with a pulse width of 7.3 ns and a peak power of over 1.7 kW at the absorbed pump power of 5.3 W.

microchip laser by further increasing the pump power. The distinct HG$_{m,n}$ modes remain stable within a certain pump power range in the passively Q-switched Nd:$YVO_4$ microchip laser; the step line and the number in brackets in figure 5 show the absorbed pump power range for distinct HG mode oscillations.

The pump power dependent repetition rate and the pulse width of the HG mode $Cr^{4+}$:YAG passively Q-switched Nd:$YVO_4$ microchip laser are shown in figure 6. The repetition rate increases linearly when the absorbed pump power is lower than 4.3 W. The repetition rate decreases by further increasing the absorbed pump power and tends to be constant when the absorbed pump power is higher than 5 W. The highest repetition rate, 31 kHz, was obtained when the absorbed pump power was 4.2 W. The decrease of the repetition rate at high pump power levels may be caused by the expansion of the laser beam area induced by the gain guide effect under gain saturation conditions. The pulse width decreases with absorbed pump power and tends to be constant when the absorbed pump power is higher than 5 W. The shortest pulse width of 7.3 ns was measured at the absorbed pump power of 5.3 W.

The variation of pulse energy and peak power with the absorbed pump power in the HG mode $Cr^{4+}$:YAG passively Q-switched Nd:$YVO_4$ microchip laser is shown in figure 7. The pulse energy and peak power increase slowly with the absorbed pump power when the absorbed pump power is lower than 4.2 W, and then increase quickly with further increase of the absorbed pump power. This is caused by the increase in the pump power intensity with pump power. The high pump power intensity under high pump power levels makes the laser mode area expand (as shown in figure 4), and the pulse energy is proportional to the laser beam area, therefore the pulse energy increases accordingly. Owing to the pulse width decreasing with the absorbed pump power (as shown in figure 6), the peak power increases with the absorbed pump power. The highest pulse energy of 12.5 $\mu$J and highest peak power of over 1.7 kW were obtained at the absorbed pump power of 5.3 W. The inset of figure 7 shows the measured laser pulse profile of the HG$_{9,8}$ mode $Cr^{4+}$:YAG passively Q-switched Nd:$YVO_4$ microchip laser at the absorbed pump power of 5.3 W. Because a large pump beam diameter was used to generate high-order HG laser modes in the $Cr^{4+}$:YAG passively Q-switched Nd:$YVO_4$ microchip laser, the pump power intensity is low. Only part of the pump area can support laser oscillation, therefore the laser beam is not well matched with the pump beam. The laser beam diameter is about 0.6 mm at an absorbed pump power of 5.3 W (as shown in figure 4), while the pump beam diameter is 1.1 mm, so only 30% of the pump beam area is used for lasing under the current experimental conditions for generating high-order HG laser modes. There is much room to improve the pulse energy in the high-order HG mode passively Q-switched Nd:$YVO_4$ microchip laser. The pulse energy can be further increased by applying a high pump power intensity to enhance the intracavity laser intensity to fully bleach the $Cr^{4+}$:YAG saturable absorber. At the same time, the peak power can be improved accordingly.

Compared to the HG modes generated in a passively Q-switched Nd:$YVO_4$ microchip laser by moving the Nd:$YVO_4$ crystal along the pump beam direction [26], the performance of high-order HG modes generated in a passively Q-switched

Nd:$YVO_4$ microchip laser has been dramatically improved by apply a 2 degree tilted large pump beam area. Various high-order HG modes such as $HG_{3,3}$, $HG_{3,6}$, $HG_{6,6}$, $HG_{12,3}$, $HG_{6,13}$, and $HG_{9,8}$ have been generated in the passively Q-switched Nd:$YVO_4$ microchip laser depending on the pump power, by applying 2 degree tilted large pump beam area pumping. The pulse energy increases by 6 times from 2 $\mu$J to 12.5 $\mu$J, and the peak power increases by more than 10 times from 130 W to 1.7 kW through proper selection of the position of the Nd:$YVO_4$ crystal along the pump beam direction (close to the focus lens and 2.4 mm from the focus spot), the incident pump beam waist, and the tilted angle of pump beam (2 degrees). The pulse energy of the high-order HG mode increases with the pump power because the laser beam area is expanded due to the gain guiding effect under high pump power.

## 4. Conclusions

Various high-order HG laser modes have been directly generated in a $Cr^{4+}$:YAG passively Q-switched Nd:$YVO_4$ microchip laser under large area, tilted laser-diode pumping when the Nd:$YVO_4$ crystal is positioned 2.4 mm away from the focus spot of the pump beam. The oscillations of the desired HG laser modes in the passively Q-switched Nd:$YVO_4$ microchip laser are controlled by manipulating the asymmetric saturated inversion population distribution inside the gain medium through varying the incident pump power. The indices of the HG laser modes increase with the pump power in the $Cr^{4+}$:YAG passively Q-switched Nd:$YVO_4$ microchip laser. A $HG_{9,8}$ mode passively Q-switched Nd:$YVO_4$ microchip laser with an average output power of 265 mW has been generated. Laser pulses with pulse widths of 7.3 ns and peak powers of over 1.7 kW working at 21 kHz have been achieved in the $HG_{9,8}$ mode passively Q-switched Nd:$YVO_4$ microchip laser. Certain HG mode passively Q-switched microchip lasers with high peak powers and high repetition rates have potential applications in optical trapping, quantum computation, and so on.

## Acknowledgments

This work was supported by the National Natural Science Foundation of China under Grants 61475130 and 61275143, and the Fundamental Research Funds for Xiamen University (20720162005).

## References

[1] Woerdemann M, Alpmann C, Esseling M and Denz C 2013 Advanced optical trapping by complex beam shaping *Laser Photon. Rev.* **7** 839–54
[2] Liu Z R, Huang K K and Zhao D M 2013 Simultaneous trapping of low- and high-index microparticles by using highly focused elegant Hermite-cosh-Gaussian beams *Opt. Lasers Eng.* **51** 761–7
[3] Chen Y F, Huang T M, Kao C F, Wang C L and Wang S C 1997 Generation of Hermite–Gaussian modes in fiber-coupled laser-diode end-pumped lasers *IEEE J. Quantum Electron.* **33** 1025–31
[4] Rigrod W W 1963 Isolation of axi-symmetrical optical-resonator modes *Appl. Phys. Lett.* **2** 51–3
[5] Rioux M, Bélanger P A and Cormier M 1977 High-order circular-mode selection in a conical resonator *Appl. Opt.* **16** 1791–2
[6] Degen C, Elsaber W and Fischer I 1999 Transverse modes in oxide confined VCSELs: influence of pump profile, spatial hole burning, and thermal effects *Opt. Express* **5** 38–47
[7] Bentley J B and Davis J A 2006 Generation of helical Ince–Gaussian beams with a liquid-crystal display *Opt. Lett.* **31** 649–51
[8] Laabs H and Ozygus B 1996 Excitation of Hermite–Gaussian modes in end-pumped solid-state lasers via off-axis pumping *Opt. Laser Technol.* **28** 213–4
[9] Lee C Y, Chang C C, Cho C Y, Tuan P H and Chen Y F 2015 Generation of higher order vortex beams from a $YVO_4$/Nd:$YVO_4$ self-Raman laser via off-axis pumping with mode converter *IEEE J. Sel. Top. Quantum Electron.* **21** 1600305
[10] Chu S-C, Ohtomo T and Otsuka K 2008 Generation of doughnutlike vortex beam with tunable orbital angular momentum from lasers with controlled Hermite–Gaussian modes *Appl. Opt.* **47** 2583–91
[11] Ohtomo T, Chu S-C and Otsuka K 2008 Generation of vortex beams from lasers with controlled Hermite– and Ince–Gaussian modes *Opt. Express* **16** 5082–94
[12] Ngcobo S, Litvin I, Burger L and Forbes A 2013 A digital laser for on-demand laser modes *Nat. Commun.* **4** 2289
[13] Dong J, Ma J, Ren Y Y, Xu G Z and Kaminskii A A 2013 Generation of Ince–Gaussian beams in highly efficient, nanosecond Cr,Nd:YAG microchip lasers *Laser Phys. Lett.* **10** 085803
[14] Dong J and Ueda K-i 2006 Observation of repetitively nanosecond pulse-width transverse patterns in microchip self-Q-switched laser *Phys. Rev.* A **73** 053824
[15] Schwarz U T, Bandres M A and Gutiérrez-Vega J C 2004 Observation of Ince–Gaussian modes in stable resonators *Opt. Lett.* **29** 1870–2
[16] Chen Y F, Lan Y P and Wang S C 2001 Generation of Laguerre–Gaussian modes in fiber-coupled laser diode end-pumped lasers *Appl. Phys.* B **72** 167–70
[17] Chen Y F and Lan Y P 2003 Observation of transverse patterns in an isotropic microchip laser *Phys. Rev.* A **67** 6
[18] Han K Z, He J L, Pan S D, Fan X W, Liu S and Wang H T 2006 Continuous transform of transverse modes and transitional status analysis in solid-state laser *Opt. Express* **14** 5295–300
[19] Eilers H, Dennis W M, Yen W M, Kuck S, Peterman K, Huber G and Jia W 1993 Performance of a Cr:YAG laser *IEEE J. Quantum Electron.* **29** 2508–12
[20] Dong J, Deng P Z, Liu Y P, Zhang Y H, Xu J, Chen W and Xie X L 2001 Passively Q-switched Yb:YAG laser with $Cr^{4+}$:YAG as the saturable absorber *Appl. Opt.* **40** 4303–7
[21] Dong J, Wang G and Cheng Y 2013 Highly efficient passively Q-switched Yb:YAG microchip lasers under high intensity laser-diode pumping *Laser Phys.* **23** 035802
[22] Sooy W R 1965 The natural selection of modes in a passive Q-switched laser *Appl. Phys. Lett.* **7** 36–7
[23] Chandonnet A, Piché M and McCarthy N 1990 Beam narrowing by a saturable absorber in a Nd:YAG laser *Opt. Commun.* **75** 123–8
[24] Ishaaya A A, Davidson N and Friesem A A 2005 Very high-order pure Laguerre–Gaussian mode selection in a passive Q-switched Nd:YAG laser *Opt. Express* **13** 4952–62
[25] Chen X M, Bai Y, Jiang M, Li L F, Zhou Y X, Wang H, Ren Z Y and Bai J T 2012 Formation of four phase-locked Gaussian beams by a saturable absorber in a neodymium-doped yttrium aluminum garnet laser *Appl. Phys. Express* **5** 122701
[26] Dong J, Bai S-c, Liu S-h, Ueda K-i and Kaminskii A A 2016 A high repetition rate passively Q-switched microchip laser for controllable transverse laser modes *J. Opt.* **18** 055205